



LAWRENCE  
LIVERMORE  
NATIONAL  
LABORATORY

# Natural CO<sub>2</sub> accumulations in the western Williston Basin: A geochemical analog for CO<sub>2</sub> Injection at the Weyburn Site

F. J. Ryerson, J. Lake, S. Whittaker, J. W. Johnson

August 23, 2012

International Journal of Greenhouse Gas Control

## **Disclaimer**

---

This document was prepared as an account of work sponsored by an agency of the United States government. Neither the United States government nor Lawrence Livermore National Security, LLC, nor any of their employees makes any warranty, expressed or implied, or assumes any legal liability or responsibility for the accuracy, completeness, or usefulness of any information, apparatus, product, or process disclosed, or represents that its use would not infringe privately owned rights. Reference herein to any specific commercial product, process, or service by trade name, trademark, manufacturer, or otherwise does not necessarily constitute or imply its endorsement, recommendation, or favoring by the United States government or Lawrence Livermore National Security, LLC. The views and opinions of authors expressed herein do not necessarily state or reflect those of the United States government or Lawrence Livermore National Security, LLC, and shall not be used for advertising or product endorsement purposes.

1  
2  
3  
4 Natural CO<sub>2</sub> accumulations in the western Williston  
5 Basin: A geochemical analog for CO<sub>2</sub> Injection at the  
6 Weyburn Site  
7  
8  
9

10 F.J. Ryerson<sup>1</sup>, John Lake<sup>2</sup>, Steven Whittaker<sup>3,4\*</sup>, James W. Johnson<sup>1,5\*</sup>  
11  
12  
13

14 <sup>1</sup>Lawrence Livermore National Laboratory, L-231, Livermore, CA 94550  
15  
16

17 <sup>2</sup>Lake Geological, Box 937, Swift Current, SK S9H 3W8  
18  
19

20 <sup>3</sup>Petroleum Technology Research Centre, 6 Research Drive  
21 Regina, SK, Canada, S4S 7J7  
22  
23

24 <sup>4</sup>Global CCS Institute, GPO Box 828, Canberra ACT 2601, Australia  
25  
26

27 <sup>5</sup>Schlumberger-Doll Research, One Hampshire St., MD-A139, Cambridge,  
28 MA 02139, USA  
29  
30  
31  
32  
33  
34  
35  
36

37 \* Current Address

38        *The Devonian carbonates of the Duperow Formation on the western flank of the Williston*  
39 *Basin in southwest Saskatchewan contain natural accumulations of CO<sub>2</sub>, and may have done*  
40 *so for as long as 50 million years. These carbonate sediments are characterized by a*  
41 *succession of carbonate cycles capped by anhydrite-rich evaporites that are thought to act as*  
42 *seals to fluid migration. The Weyburn CO<sub>2</sub> injection site lies 400 km to the east in a series of*  
43 *Mississippian carbonates that were deposited in a similar depositional environment. That*  
44 *natural CO<sub>2</sub> can be stored long-term within carbonate strata has motivated the investigation*  
45 *of the Duperow rocks as a potential natural analogue to storage of anthropogenic CO<sub>2</sub> that*  
46 *may ultimately provide additional confidence for CO<sub>2</sub> sequestration in carbonate lithologies.*  
47 *For the Duperow strata to represent a legitimate analog for Midale injection and storage, the*  
48 *similarity in lithofacies, whole rock compositions, mineral compositions and porosity with the*  
49 *Midale Beds must be established. Here we compare lithofacies, whole rock compositions,*  
50 *mineralogy and mineral compositions from both locales. The major mineral phases at both*  
51 *locales are calcite, dolomite and anhydrite. In addition, accessory pyrite, fluorite, quartz and*  
52 *celestine (strontium sulfate) are also observed. Dawsonite is not observed within the CO<sub>2</sub>-*  
53 *bearing horizons of the Duperow Formation, however. The distribution of porosity in the*  
54 *Midale Vuggy units is virtually identical to that of the Duperow Formation, but the Marly units*  
55 *of the Midale have significantly higher porosity. The Duperow Formation is topped by the*  
56 *Dinesmore evaporite that is rich in anhydrite, and often contains authigenic K-feldspar. The*  
57 *chemistry of dolomite and calcite from the two localities also overlaps. Silicate minerals are in*  
58 *low abundance within the analyzed Duperow samples, < 3 wt% on a normative basis, with*  
59 *quartz the only silicate phase identifiable in x-ray diffraction patterns. The Midale Beds*  
60 *contain significantly higher silica/silicate concentrations, but the silicate minerals observed,*  
61 *K-feldspar and quartz, are unlikely to participate in carbonate mineral precipitation due to*  
62 *the absence of alkaline earths. Hence, physical and solution trapping are likely to be the*  
63 *primary trapping mechanisms at both sites. Given the similarity of mineral constituents,*  
64 *whole rock and mineral chemistry, reactive transport models developed for the Weyburn site*  
65 *should also be applicable to the Duperow lithologies.*

## 66    **1.    Introduction**

67        Long-term isolation of anthropogenic carbon dioxide requires predictions that extend  
68 beyond the temporal and spatial scale of laboratory experiments and approaches those of  
69 natural geologic processes. Whether the various isolation scenarios reach their  
70 thermodynamic endpoints remains speculative, however.    Natural analogs, geologic

71 settings that mimic processes anticipated in engineered waste isolation operations, provide  
72 an opportunity to evaluate the extrapolation of experimental results. Natural analogs are  
73 most useful in characterizing the effects of rock-water interaction that depend on mineral-  
74 fluid dissolution and precipitation kinetics. For instance, equilibrium models of CO<sub>2</sub>  
75 injection in silica-rich saline aquifers predict carbonate mineral precipitation that depends  
76 upon a coupled process in which the alkaline earths required to form carbonate minerals  
77 are supplied by, and hence rate-limited by, silicate mineral dissolution (Johnson et al.,  
78 2002). If silicate mineral dissolution is sufficiently sluggish, carbonate precipitation will  
79 not occur in spite of thermodynamic predictions. A number of natural accumulations of the  
80 carbon dioxide have been identified and lend confidence to the potential for long-term  
81 geologic sequestration of anthropogenic carbon dioxide. These settings also provide an  
82 opportunity to evaluate the long-term influence of CO<sub>2</sub> storage on the mineralogy and  
83 geochemistry of the host carbonates (Gilfillan et al., 2008; Gilfillan et al., 2009; Gilfillan et al.,  
84 2011 ; Kaszuba et al., 2010; Kaszuba et al., 2011 ; Pearce, 2006).

85 Exploratory drilling in the western Williston Basin encountered natural accumulations  
86 of CO<sub>2</sub>, N<sub>2</sub> and He within the clastic strata of the Cambrian Deadwood Formation and in the  
87 carbonates of the Middle Devonian Winnipegosis and Souris River and Upper Devonian  
88 Duperow Formations (Figure 1). These natural CO<sub>2</sub> occurrences are found about 400 km  
89 west of the site of the IEA Weyburn CO<sub>2</sub> Storage and Monitoring Project (Figure 1), and in  
90 some cases contain as much as 80 mol% CO<sub>2</sub> within the Middle and Upper units of the  
91 Wymark Member (Lane, 1987). At the Weyburn Field CO<sub>2</sub> is being injected into  
92 Mississippian Midale Beds, a succession of cyclic carbonate deposits formed in a shallow  
93 setting with porous intervals capped by evaporite units of variable thickness that are  
94 thought to be effective seals to fluid migration. Previous workers have demonstrated the  
95 depositional and stratigraphic similarity between the Midale Beds and the Devonian  
96 carbonates to the west (Lake and Whittaker, 2006). In this paper we present mineralogical  
97 and geochemical data from drill cores in these Devonian carbonates for comparison with  
98 those of the Midale beds.

## 99 **2. Regional Geology**

### 100 **2.1 Duperow-Weyburn Reservoir Comparison**

101 Carbonates of the Devonian Duperow Formation are now included as deposits within  
102 the Williston Basin, which is an elliptical depression about 560 km in diameter and centered

103 in North Dakota (Figure 1), but these shallow platform carbonates and evaporites were  
104 initially formed along the eastern margin of the Devonian Elk Point Basin (Moore, 1989).  
105 The Elk Point Basin trended northwest and was bounded by the Precambrian Shield margin  
106 in the east, the Transcontinental Arch to the south, and open circulation to the northwest.  
107 Common consensus states that a Precambrian positive feature existed immediately south of  
108 the study area in northern Montana, based on onlap and thinning of the Devonian  
109 Winnipegosis and Dawson Bay formations (Figure 2) onto this feature. The basal Duperow  
110 strata south of this area are thin or absent as a result of onlap (Kent, 1968) (Pilatzke et al.,  
111 1987) (Burke and Heck, 1988). Subsequent crustal and basinal downwarping resulted in  
112 the present study area being included in the western portion of the Williston Basin by  
113 Mississippian time. The structure of western North America has been influenced by crustal  
114 shortening associated with the Antler Orogeny which was centered in Nevada during the  
115 Upper Devonian–Early Mississippian (Goebel, 1991). Further crustal shortening and  
116 uplift occurred in western North America during the massive Cordilleran Orogeny during  
117 the early Tertiary. Locally, the major structural elements include the Sweetgrass–North  
118 Battleford Arch over the inter-provincial border with Alberta (Kent, 1968). The structure  
119 map of the Duperow Formation is shown in Figure 3 along with other structural elements  
120 and the locations and formations in which inert gases have been detected in  
121 southwestern Saskatchewan. Significant local structural uplift is associated with Tertiary  
122 alkalic intrusives in the Bearpaw Mountains, Little Rocky Mountains, and Bowdoin Dome  
123 intrusions in northern Montana (see Figures 2 and 3). These intrusives have been dated at 50 my  
124 (Eocene) (Marvin et al., 1973).

125 The Upper Devonian Duperow Formation in southwestern Saskatchewan shows facies  
126 variability both laterally and vertically that results in thin, widespread depositional cycles  
127 that are suggestive of a stable cratonic and climatic environment. For example, individual  
128 markers within the Duperow may be correlated for 160 km across the basin center (Burke  
129 and Heck, 1988). Duperow strata generally exhibit shallowing upward cycles of carbonate  
130 deposition in very shallow settings that may be capped by evaporite formation.  
131 These anhydrite layers at the top of individual cycles are considered to be effective seals to  
132 fluid migration. The cycles are broadly similar to those observed in the Mississippian strata  
133 of the Weyburn Pool, but the Mississippian cycles show more rapid fluctuations in sea level  
134 and, consequently, more exposure surfaces (Burrowes, 2001). The shallow peritidal  
135 depositional setting, however, was similar for each location.

136 The geological setting of the Devonian Duperow Formation in southwestern  
137 Saskatchewan is quite similar to that of the Mississippian Midale Beds of the Weyburn Pool  
138 in southeastern Saskatchewan (Figure 4). The strata are largely continuous between the  
139 regions, although the Mississippian Midale Beds have been truncated by the Sub-Mesozoic  
140 Unconformity surface in the western portion of the basin. Duperow strata, however, are  
141 present and are essentially laterally continuous at both locations, with the exception of  
142 some karstification and erosion associated with the Wymark Middle Member. At each  
143 location, the CO<sub>2</sub>-bearing units are overlain by approximately 1500 m of clastic Mesozoic strata  
144 that contain several thick shale sequences that are highly effective aquitards

145 The reservoir system in the Weyburn Field is a combination of stratigraphic, diagenetic,  
146 hydrodynamic, and structural traps. The Mississippian Midale Beds pinch out at the Sub-  
147 Mesozoic Unconformity where diagenesis has also occurred to markedly reduce porosity.  
148 The reservoir layers are sealed by the Midale Evaporite, a 2 to 11 m thick anhydrite layer  
149 formed in a restrictive, salina-like environment. The reservoir layers are shallow, peritidal  
150 carbonate deposits that have been variably dolomitized. The lower Midale Vuggy unit is a  
151 limestone that has about 2 to 15% porosity, whereas the upper Midale Marly unit is a  
152 dolostone that has an average of about 27% porosity.

153 The traps in Duperow strata are mainly related to structures formed by dissolution of  
154 underlying salt layers. The porous layers within the Duperow, however, are sealed by  
155 variably thick (usually greater than 2 m) anhydrite layers, such as the Dinsmore Evaporite,  
156 that formed in restricted environments. The reservoir layers are generally limestones to  
157 slightly dolomitized limestones formed in a low-energy, shallow carbonate shelf  
158 environment. The reservoirs often exhibit vuggy porosity and, although core analyses are  
159 not abundant, measured porosities for the reservoir units range from 6 to 18%.

## 160 2.2 CO<sub>2</sub> and Inert Gas Distribution

161 Exploratory drilling in the Duperow Formation reported CO<sub>2</sub> and inert (He and N<sub>2</sub>) gas  
162 potential in the study area (Figure 3). The highest concentrations of natural CO<sub>2</sub> (~80%) in  
163 the Duperow formation are found in samples at depths greater than 1500 m (Table 1)  
164 where pressure and temperature exceed the critical point of CO<sub>2</sub> (30.98°C, 7.38 MPa). It has  
165 been suggested that subsurface CO<sub>2</sub> and inert gas occurrences are related to the migration  
166 of gas into overlying aquifers from underlying igneous activity (Stevens et al., 2001) (Moore  
167 et al., 2003). Kent and Kreis (2001) recognized anomalously high geothermal gradients in  
168 Mississippian Lodgepole Formation oil wells along the Battle Creek–Rangeview Structure in  
169 which heavy oil (10 degree API gravity) flows to surface. The high geothermal gradient  
170 likely results from the igneous activity in Montana. Alkalic intrusives were emplaced in  
171 Montana approximately 50 my ago (Marvin et al., 1973) during igneous activity associated  
172 with the Bearpaw Mountains, Little Rocky Mountains, and potentially also with the Bowdoin  
173 Dome (Figure 2). Carbon dioxide and inert gases (N<sub>2</sub> and He) have been detected in the  
174 clastic Cambrian Deadwood Formation, and the carbonate Middle Devonian Dawson Bay  
175 and Winnipegosis formations, and the Upper Devonian Duperow Formation. If reaction of  
176 limestones with alkalic intrusions generated the CO<sub>2</sub> or if the inert gases are  
177 directly associated with the igneous source, the lateral migration path would have been  
178 around 100 km (Figure 2).

179 Creany *et al.* (1994) suggest that migration and maturation of hydrocarbons occurred in  
180 the Western Canada Sedimentary Basin during the Late Cretaceous and Early Tertiary  
181 (Palaeocene) due to burial and thrusting associated with mountain building along the  
182 western margin of North America (Cordilleran Orogeny). Because the Devonian section in  
183 Saskatchewan is immature with respect to hydrocarbon generation due to the shallow  
184 burial history of the area, hydrocarbons did not migrate into the porous reservoirs of  
185 southwest Saskatchewan until uplift in the Rocky Mountains. Hydrocarbon migration in  
186 southwest Saskatchewan occurred prior to alkalic igneous activity so that inert gas  
187 migration would have occurred after oil migration. If any hydrocarbons were present  
188 in these reservoirs, and minor staining has been observed, it may be possible that the inert  
189 gases displaced them. Regardless, the gases have likely been in the Duperow reservoirs  
190 since the Tertiary (Palaeocene), or for about 50 my.

191 The CO<sub>2</sub> interval in the well containing the most CO<sub>2</sub> in the Duperow Formation (well 4-

192 31-3-26W3 tested almost 83% CO<sub>2</sub> in the top of the Wymark Middle Member) was never  
193 produced and was plugged in 1955. In 2001, a new well was drilled at the same location to  
194 exploit a shallower natural gas occurrence within the Jurassic Upper Shaunavon Formation  
195 at around 800 m depth. Gas tested from the new well contains only trace amounts of  
196 CO<sub>2</sub>. Moreover, in the immediate vicinity of the CO<sub>2</sub> deposit, gas-receiving stations, which  
197 essentially serve to integrate gas from a number of shallower wells, do not contain  
198 measurable amounts of CO<sub>2</sub>. It is inferred, therefore, that leakage from natural CO<sub>2</sub>  
199 reservoirs into shallower horizons in southwestern Saskatchewan has not been  
200 significant during the past 50 million years.

### 201 **3. Mineralogy and Geochemical Characterization**

202 Sample well locations and depths, along with the CO<sub>2</sub> concentrations in the drillstem gas  
203 samples are given in Table 1. Electron microprobe analysis was performed on the same  
204 polished thin sections characterized petrographically by Lake and Whittaker (2006). In  
205 addition we retrieved bulk samples for adjacent core for XRF and XRD analysis.

#### 206 **3.1 Analytical Methods**

207 The XRF analyses were performed at the XRF laboratory at Michigan State University.  
208 Analyses were performed on a Bruker S4 PIONEER, a 4 kW wavelength dispersive X-ray  
209 fluorescence spectrometer (WDXRF). The S4 PIONEER with advanced 4 kW tube provides  
210 highest sensitivity especially for light elements and trace elements due to optimized beam  
211 geometry and very thin Beryllium XRF tube window used in combination with software  
212 optimized excitation parameters for each element analyzed. Data reduction is performed  
213 with Bruker's SPECTRAplus software using fundamental parameters. The samples were  
214 prepared by fusion and Li-tetraborate. The samples were analyzed for Si, Al, Fe, Mn, Mg, Ca,  
215 Na, K, P and S, along with trace elements Cr, Ni, Cu, Zn, Rb, Sr, Y, Nb, Ba and La. Sr was the  
216 only trace element routinely above detection limits. The analyses are given in Table 2. The  
217 high "loss on ignition" (LOI) reflect the loss of CO<sub>2</sub> during fusion. Analyses are typically  
218 within 2% of standard values on a relative basis.

219 X-ray powder diffraction analysis performed on a Rigaku Geigerflex D-MAX/A  
220 Diffractometer using Cu-Ka radiation in the Dept. on Earth and Planetary Sciences at  
221 Washington University. The instrument is equipped with a vertical goniometer and a  
222 scintillation counter. Analyses were obtained at 35kV and 35mA and acquired using PC-

223 based Datascan software and processed using Jade software

224 Electron microprobe analyses were performed on a JEOL-8200 at Lawrence Livermore  
225 National Laboratory. The instrument was operated at 15 kV with a beam current of 5 na  
226 and a 5  $\mu\text{m}$  diameter spot. Higher beam currents resulted in beam damage to some of the  
227 carbonate minerals. Analysis locations were obtained in the following sequence: (1) a  
228 “synoptic” backscattered electron map was obtained for the entire thin section at by  
229 assembling 40X maps into a mosaic, x-ray maps were also acquired to search for minor  
230 phases of interest such as dawsonite, (2) the synoptic maps were then used to establish an  
231 analysis grid for point-by-point analysis of the sample. (3) The synoptic maps were used to  
232 locate area of interest from which higher magnification backscattered electron maps and x-  
233 ray maps were acquired. (4) Point analyses were obtained in areas where mineral zoning  
234 was observed.

### 235 **3.2 Petrography**

236 Durocher *et al.* (2003) performed an extensive analysis of the mineralogy, phase  
237 compositions and whole rock chemistry of samples from the Midale Formation. These  
238 samples were collected prior to CO<sub>2</sub> injection and serve as the CO<sub>2</sub>-free baseline for  
239 comparison with the CO<sub>2</sub>-bearing samples from the Duperow formation analyzed here.

240 The Duperow and Midale samples are largely limestones and dolostones with a simple  
241 mineralogy consisting of calcite, dolomite and anhydrite. Lake and Whittaker (2006)  
242 documented the petrographic similarity of the samples from Duperow and Midale units,  
243 consistent with their common depositional setting. The carbonate rocks from both locations  
244 can be roughly classified as dolomitized mudstones, fossiliferous limestones, pelletal lime  
245 mudstones (Figure 5 and 6) and evaporites (Figure 7). Pyrite and fluorite are also common  
246 accessory minerals (Figure 5), and some anhydrite-rich assemblages contain celestine as  
247 well (Figure 6). Equilibrium calculations (Bethke and Yeakel, 2009) performed for calcite,  
248 dolomite, anhydrite bearing assemblages in equilibrium with Midale brine compositions  
249 (Cantucci *et al.*, 2009) indicate that celestine expected as a common accessory phase. The  
250 abundance of silicate minerals in the Duperow samples is low, < 3 wt% with quartz the  
251 most common silicate phase (Figure 8). Durocher *et al.* (2003) analyzed a larger suite of  
252 Midale samples and found normative quartz concentrations as high as 30 wt% in some  
253 samples. K-Feldspar is largely restricted to evaporate horizons, and is often found as

254 inclusions in anhydrite. Dawsonite was not observed petrographically, in backscattered  
255 electron maps or in the Na and K x-ray maps from any of the analyzed samples.

### 256 3.3 Whole Rock Geochemistry

257 The major element data for the Midale units are taken from Durocher *et al.* (2003). At  
258 both locations, the samples consist of calcite, dolomite, anhydrite and variable  
259 concentrations of silicate minerals, the overall chemical variability is best displayed as  
260 variations in CaO, MgO, SO<sub>2</sub> and SiO<sub>2</sub> (Figure 9). Since anhydrite (CaSO<sub>3</sub>) was the major  
261 sulfur-bearing phase, all sulfur was “oxidized” to yield SO<sub>2</sub> to simplify comparison. The  
262 variation in CaO-MgO-SO<sub>2</sub> clearly displays the mixing of calcite, dolomite and anhydrite,  
263 with essentially all analyses falling in compositional region defined by these phases (Figure  
264 9a). The Midale data extends further toward the CaO-SO<sub>2</sub> join, indicative of a larger fraction  
265 of evaporite samples in that data set. The FeO concentrations in both suites are similar  
266 (Figure 9b). The range of Duperow samples is much more restricted in terms of CaO-MgO-  
267 SiO<sub>2</sub> lying along the CaO-MgO join (Figure 9c). The Midale samples in general contain a  
268 higher proportion of silica than the Duperow, and this is shown by the large number of  
269 samples falling on a join radial to the SiO<sub>2</sub> apex, consistent with a higher detrital component  
270 in the Midale samples. It is difficult to assess whether the higher SiO<sub>2</sub> concentrations  
271 represents sampling bias or a true difference between the depositional environments.

### 272 3.4 Carbonate Mineral Chemistry

273 Carbonate mineral chemistry was determined by electron microprobe analysis for the  
274 Midale Beds and Duperow Formation (Durocher *et al.*, 2003; Ryerson and Johnson, 2010,  
275 respectively), and are not tabulated here. The major carbonate endmember components  
276 are calcite, dolomite and ankerite, allowing the variation in calcite and dolomite chemistry  
277 to be displayed on the Ca-Mg-Fe ternary in terms of cations (Figure 10). The carbonates  
278 from the Midale Beds lie almost entirely along the Ca-Mg join consistent with low  
279 concentrations of Fe in these carbonates. The Duperow analyses are similarly restricted to  
280 the Ca-Mg join, but there is a small population of samples trending to higher Fe  
281 concentrations toward ankerite. As the whole rock chemistry displays little variation in FeO  
282 concentration, the higher Fe-dolomites from Duperow likely reflect higher density of  
283 sampling, including Fe-rich rim compositions from dolomites adjacent to pores (Figure 11).  
284 These rim compositions likely reflect growth from late stage fluids enriched in incompatible  
285 elements. The sampling of Fe-rich dolomites from the Duperow is also displayed in

286 histograms of the Mg/(Mg+Ca) ratio for carbonate compositions as a “tail” toward lower  
287 values reflecting the substitution of Fe for Mg (Figure 12).

### 288 3.5 Porosity

289 The ability to store and trap natural and anthropogenic CO<sub>2</sub> is directly related to the  
290 distribution of porosity in the reservoirs. This is especially true in the case of physical  
291 entrapment or solution trapping where the CO<sub>2</sub>-bearing fluid/gas phase is free to migrate.  
292 Porosity data, obtained from the Ministry of Energy and Resources (courtesy of Erik Nickel)  
293 are shown in Figure 13. The Midale beds display a bimodal porosity distribution associated  
294 with the lower porosity Vuggy (average ~ 0.1) and the higher porosity Marly units (average  
295 ~ 0.25). While the data for the Duperow formation are less abundant, the porosity closely  
296 resembles that of the Vuggy unit at Weyburn with an average of ~ 0.12 with some values  
297 reaching as 0.35.

## 298 4. Discussion

299 Based upon the age of potential sources of CO<sub>2</sub> and the absence of CO<sub>2</sub> at shallower  
300 depths, it is inferred that the Duperow Formation has trapped natural CO<sub>2</sub> for at least 50  
301 million years. The Mississippian Midale Beds and Devonian Duperow Formations were  
302 deposited under similar environmental conditions producing a succession of thin carbonate  
303 cycles intercalated with anhydrite-rich evaporates. The carbonates are primarily  
304 limestones and dolostones, rich in calcite and dolomite, with variable amounts of silicate  
305 minerals and accessory pyrite, fluorite and celestine. Petrographic analysis established the  
306 correspondence of specific lithofacies at both sites. The porosity distributions are similar,  
307 although the Marly unit of Midale beds does have a significantly higher porosity than  
308 carbonates of the Duperow formation. The major element and mineral chemistry of the two  
309 stratigraphic successions are also similar. The one compositional factor distinguishing the  
310 successions is the higher concentration of silica and silicate minerals in the Midale beds. It  
311 should be noted that quartz and K-feldspar are the only silicate minerals identified in thin  
312 section in the Duperow or Midale Beds. Silicate minerals rich in alkaline earths, such as  
313 plagioclase, appear in normative calculations (Durocher *et al.*, 2003) but have not be  
314 identified in thin section.

315 Using fluid sample chemistry and observed mineral assemblages, Cantucci *et al.*, (2009)  
316 reconstructed the pre-injection reservoir fluid compositions at the Weyburn site. They then

317 assessed the mineral-fluid evolution of the reservoir during CO<sub>2</sub> injection, concluding that  
318 safe, long-term storage of CO<sub>2</sub> could be accomplished through a combination of solubility  
319 trapping and mineral trapping due to the precipitation of dawsonite, NaAlCO<sub>3</sub>(OH)<sub>2</sub>. The  
320 absence of dawsonite in samples containing high CO<sub>2</sub> concentrations within the Duperow  
321 Formation indicate that dawsonite is either chemically unstable, or that precipitation is  
322 kinetically limited even on the scale of tens of millions of years (see Hellevang et al., 2011).  
323 While carbonate mineral precipitation does not appear to have occurred within the  
324 Duperow Formation, CO<sub>2</sub> does appear to have been effectively trapped by these lithologies  
325 without aid of mineral trapping.

326 Unfortunately, we do not have access to fluid compositions from the CO<sub>2</sub>-bearing  
327 Duperow Formation horizons, and cannot quantitatively assess the extent of solubility  
328 trapping. However, Kaszuba *et al.* (2011) investigated a very similar suite of natural analog  
329 samples from the Madison Limestone in Wyoming obtaining mineral and fluid geochemical  
330 data from wells outside and within the area of supercritical CO<sub>2</sub> accumulation. The natural  
331 CO<sub>2</sub> storage is estimated to be 50 million years, similar to the estimated storage interval for  
332 the Duperow Formation. With the exception of native sulfur observed in the Madison  
333 Limestone, the mineralogy is essentially identical to that of both the Duperow Formation  
334 and the Midale beds. Like the Duperow Formation, dawsonite is not observed within the  
335 areas of CO<sub>2</sub> accumulation in the Madison Limestone. Suppressing dawsonite formation,  
336 geochemical modeling of the Madison limestone-brine system yields results that are similar  
337 to those observed in the fluid compositions and mineralogy of the CO<sub>2</sub>-free and -bearing  
338 lithologies (Kaszuba et al., 2011). Given the comparable age, lithology and depths at the  
339 Madison Limestone and the Duperow Formation, it is likely that fluid-gas equilibrium was  
340 attained with the Duperow, and that CO<sub>2</sub> trapping is achieved through both solubility and  
341 physical trapping mechanisms.

342 In general, mineral trapping of CO<sub>2</sub> will be largely dependent upon the dissolution of  
343 alkaline earth-bearing silicate minerals to provide the cations necessary for formation of  
344 carbonates. For carbonate reservoirs, CO<sub>2</sub> injection results primarily in decreased pH  
345 accompanied by carbonate mineral dissolution. The predicted dawsonite precipitation  
346 reflects that high sodium concentration of reservoir brines as the lithologies themselves  
347 tend to be poor in sodium. The absence of precipitated carbonate minerals in both the  
348 Williston and Wyoming limestone/dolostone natural analogs would appear to preclude

349 mineral trapping in CO<sub>2</sub> injection sites of similar lithology, such at the Weyburn-Midale  
350 injection site. That the concentration of silicate minerals is higher in the Midale Beds than  
351 in the Duperow Formation will not enhance its potential for mineral trapping due to the  
352 nature of the silicate minerals present.

353 The Duperow Formation in which natural accumulations of CO<sub>2</sub> are observed is very  
354 similar to the Midale Beds in terms of whole rock chemistry, mineralogy, mineral chemistry  
355 and porosity distribution. In both cases, anhydrite-rich evaporates, sometimes contains  
356 authigenic K-feldspar, form aquitards which, in the case, of the Duperow appear to have  
357 prevented loss of CO<sub>2</sub> over a time frame that may extend as long as 50 million years. (cf,  
358 Lake and Whittaker, 2006). These accumulations, coupled with the striking similarity  
359 between these lithologies, provide support for the security of CO<sub>2</sub> injection at Weyburn.

## 360 **Acknowledgements**

361 This work performed under the auspices of the U.S. Department of Energy by Lawrence  
362 Livermore National Laboratory under Contract DE-AC52-07NA27344. The authors are  
363 grateful for analytical support from Thomas Vogel (XRF, Michigan State) and Paul Carpenter  
364 (XRD, Washington University) and to Erik Nickel for providing porosity data for the  
365 Duperow Formation. This work was supported by the Petroleum Technology Research  
366 Centre.

367

## 368 **References**

- 369 Bethke, C.M., Yeakel, S., 2009. The Geochemist's Workbench Release 8.0: Reaction Modeling  
370 Guide. University of Illinois., Champaign, Illinois.
- 371 Burke, R.B., Heck, T.J., 1988. Reservoir characteristics of the Duperow Formation at Tree  
372 Top Field, North Dakota, in: Goolsby, S.M., Longman, M.W. (Eds.), Occurrence and  
373 Petrophysical Properties of Carbonate Reservoirs in the Rocky Mountain Region. Rky.  
374 Mtn. Assoc. Geol., Denver, pp. 303-316.
- 375 Burrowes, G., 2001. Investigating CO<sub>2</sub> storage potential of carbonate rocks during tertiary  
376 recovery from a billion barrel oil field, Weyburn, Saskatchewan: Part 2 - reservoir  
377 geology (IEA Weyburn CO<sub>2</sub> Monitoring and Storage Project), Summary of Investigations  
378 2001. Saskatchewan Geological Survey, pp. 455-468.
- 379 Cantucci, B., Montegrossi, G., Vaselli, O., Tassi, F., Quattrocchi, F., Perkins, E.H., 2009.  
380 Geochemical modeling of CO<sub>2</sub> storage in deep reservoirs: The Weyburn Project (Canada)  
381 case study. *Chemical Geology* 265, 181-197.
- 382 Creany, S., Allen, J., Cole, K.S., Fowler, M.G., Brooks, P.W., Osadetz, K.G., MacQueen, R.W.,  
383 Snowdon, L.R., Riediger, C.L., 1994. Petroleum Generation and Migration in the Western  
384 Canada Sedimentary Basin, in: Mossop, G.D., I., S. (Eds.), Geological Atlas of the Western  
385 Canada Sedimentary Basin, Can. Soc. Petrol. Geol./ Alta. Resear. Council, Calgary, pp.

- 386 455-468.
- 387 Durocher, K., Hutcheon, I., Shevalier, M., Gunter, B., Perkins, E., Bloch, J., 2003. Subtask 3.1;  
388 Reservoir (Baseline) Mineralogy Final Report, in: Project, I.W.C.M.a.S. (Ed.).
- 389 Gilfillan, S.M., Ballentine, C.J., Holland, G., Blagburn, D., Lollar, B.S., Stevens, S., Schoell, M.,  
390 Cassidy, M., 2008. The noble gas geochemistry of natural CO<sub>2</sub> gas reservoirs from the  
391 Colorado Plateau and Rocky Mountain provinces, USA. *Geochimica Et Cosmochimica*  
392 *Acta* 72, 1174-1198.
- 393 Gilfillan, S.M.V., Lollar, B.S., Holland, G., Blagburn, D., Stevens, S., Schoell, M., Cassidy, M.,  
394 Ding, Z., Zhou, Z., Lacrampe-Couloume, G., Ballentine, C.J., 2009. Solubility trapping in  
395 formation water as dominant CO<sub>2</sub> sink in natural gas fields. *Nature* 458, 614-618.
- 396 Gilfillan, S.M.V., Wilkinson, M., Haszeldine, R.S., Shipton, Z.K., Nelson, S.T., Poreda, R., 2011.  
397 He and Ne as tracers of natural CO<sub>2</sub> migration up a fault from a deep reservoir.  
398 *International Journal of Greenhouse Gas Control* 5, 1507-1516.
- 399 Goebel, K.A., 1991. Paleogeographic setting of late Devonian–early Mississippian transition  
400 from passive to collisional margin Antler Foreland, eastern Nevada and western Utah;;  
401 in: Cooper, J.D., Stevens, C.H. (Eds.), *Paleozoic Paleogeography of the Western United*  
402 *States-11. Pacific Section SEPM*, pp. 401-418.
- 403 Hellevang, H., Declercq, J., Aagaard, P., 2011. Why is Dawsonite Absent in CO<sub>2</sub> Charged  
404 Reservoirs? *Oil & Gas Science and Technology-Revue D Ifp Energies Nouvelles* 66, 119-  
405 135.
- 406 Johnson, J.W., Nitao, J.J., Steefel, C.I., 2002. Fundamental elements of geologic CO<sub>2</sub>  
407 sequestration in saline aquifers. *Abstr Pap Am Chem S* 223, U568-U568.
- 408 Kaszuba, J.P., Navarre-Sitchler, A., Thyne, G., Chopping, C., 2010. A natural analogue in  
409 Southwest Wyoming for geologic co-sequestration of carbon & sulfur. *Geochimica Et*  
410 *Cosmochimica Acta* 74, A498-A498.
- 411 Kaszuba, J.P., Navarre-Sitchler, A., Thyne, G., Chopping, C., Meuzelaar, T., 2011. Supercritical  
412 carbon dioxide and sulfur in the Madison Limestone: A natural analog in southwest  
413 Wyoming for geologic carbon-sulfur co-sequestration. *Earth and Planetary Science*  
414 *Letters* 309, 131-140.
- 415 Kent, D.M., 1968. *The Geology of the Upper Devonian Saskatchewan Group and Equivalent*  
416 *Rocks in Western Saskatchewan and Adjacent Areas*;. *Sask. Dep. Miner. Resour.*, p. 224p.
- 417 Kent, D.M., Kreis, L.K., 2001. Mississippian Madison Formation low-gravity oilfields in  
418 southwestern Saskatchewan: Examples of unconformity diagenesis controlling  
419 reservoir quality;,. *Summary of Investigations 2001. Saskatchewan Geological Survey*,  
420 pp. 46-55.
- 421 Lake, J., Whittaker, S., 2006. Occurrences of CO<sub>2</sub> within Southwest Saskatchewan: Natural  
422 Analogues to the Weyburn CO<sub>2</sub> Injection Site, *Summary of Investigations, 2006.*  
423 *Saskatchewan Geologic Survey*, pp. 1-14.
- 424 Lane, D.M., 1987. *Subsurface Carbon Dioxide in Saskatchewan: Sources and Potential Use in*  
425 *Enhanced Oil Recovery. Saskatchewan Energy and Mines*, p. 40.
- 426 Marvin, R.F., Witkind, I.J., Keefer, R.W., Mehnert, H.H., 1973. Radiometric Ages of Intrusive  
427 Rocks in the Little Belt Mountains, Montana. *Geol. Soc. Amer. Bull.* 84, 1977-1986.
- 428 Moore, J., 1989. *The Kaskaskia Sequence: Reefs, Platforms and Foredeeps. The Lower*

429 Kaskaskia Sequence – Devonian, in: Ricketts, B.D. (Ed.), Western Canada Sedimentary  
430 Basin: A Case History. Can. Soc. Petrol. Geol., pp. 139-164.

431 Moore, J., Adams, M., Allis, R., Lutz, S., Rauzi, S., 2003. CO<sub>2</sub> mobility in natural resources  
432 beneath the Colorado Plateau and southern Rocky Mountains: An example from the  
433 Springerville–St. Johns Field, Arizona and New Mexico, Second Annual Conference on  
434 Carbon Sequestration. U.S. Dept. Energy, Alexandria, VA, p. 22p.

435 Pearce, J.M., 2006. What can we learn from natural analogues? - An overview of how  
436 analogues can benefit the geological storage of CO<sub>2</sub>. Advances in the Geological Storage  
437 of Carbon Dioxide: International Approaches to Reduce Anthropogenic Greenhouse Gas  
438 Emissions 65, 129-139.

439 Pilatzke, R.H., Fischer, D.W., Pilatzke, C.L., 1987. Overview of Duperow (Devonian)  
440 production in the Williston Basin, in: J.A., P., D.M., K., S.B., A., R.H., P., M.W., L. (Eds.),  
441 Williston Basin: Anatomy of a Cratonic Oil Province. Rky. Mtn. Assoc. Geol., Denver, pp.  
442 423-432.

443 Ryerson, F.J., Johnson, J.W., 2010a. Characterization of the Wymark CO<sub>2</sub> Reservoir: A Natural  
444 Analog to Long-Term CO<sub>2</sub> Storage at Weyburn. Lawrence Livermore National  
445 Laboratory, Livermore, CA, p. 121.

446 Ryerson, F.J., Johnson, J.W., 2010b. Comparison of the Wymark CO<sub>2</sub> Reservoir with the  
447 Midale Beds at the Weyburn CO<sub>2</sub> Injection Project. Lawrence Livermore National  
448 Laboratory, Livermore, CA, p. 11.

449 Stevens, S.H., Pearce, J.M., Rigg, A.A.J., 2001. Natural analogs for geologic storage of CO<sub>2</sub>: An  
450 integrated global research program, First National Conference on Carbon Sequestration.  
451 U.S. Dept. Energy,, Alexandria, VA, p. 12p.

452

453

454

Table 1. Sample core locations and mineralogy

<i>Wymark core</i>	Well	Unit	Mineralogy	Mol% CO <sub>2</sub>
3-10-14-14-W3M 5555	T.W. Wymark #1	Wymark Middle	Cal, Do (Fl)	-
3-10-14-14-W3M 5627	T.W. Wymark #1	Wymark Middle	Anhy, Do, Cal	-
4-14-18-16 W3M 4827	Norcanoil Pennant	Wymark Upper	Do, Cal, (Qtz)	-
4-31-3-26 W3M 5163	Imp. Battle Cr.	Wymark Upper	Do, Anhy, (Py)	81.3
4-31-3-26 W3M 5164	Imp. Battle Cr.	Wymark Upper	Do, Anhy, (Py)	81.3
4-31-3-26 W3M 5627	Imp. Battle Cr.	Wymark Middle	Cal, Do, Anhy (Fl)	81.3
4-31-3-26 W3M 5632	Imp. Battle Cr.	Wymark Middle	Cal, Do, Anhy	82.6
4-31-3-26 W3M 5642	Imp. Battle Cr.	Wymark Middle	Cal, Do, (Py)	-
5-7-14-10 W3M 5288	Braddock	Wymark Upper	Anhy, Cal, Do, (Py), (Ksp)	-
5-7-14-10 W3M 5413	Braddock	Wymark Upper	Do, Anhy, SrSO <sub>3</sub> , (Py)	-
10-32-183 W3M 4596	Parkbeg Cr #1	Upper Birdbear	Do, Anhy, (Fl)	-
10-32-183 W3M 4639	Parkbeg Cr #1	Lower Birdbear	Do, Anhy, (Py), (Ksp)	-
10-32-183 W3M 4645	Parkbeg Cr #1	Lower Birdbear	Do, Anhy, (Py), (Ksp)	-
10-32-183 W3M 4746	Parkbeg Cr #1	Basal Seward B.	Do, (Py), (Ksp)	-
10-32-183 W3M 4813	Parkbeg Cr #1	Basal Seward A	Do, Cal, Anhy, SrSO <sub>3</sub> , (Py)	-
<i>Eastend Core</i>				
15-11-6-20 W3M 6014	T.W. Eastend Cr. #1	Wymark Upper	Anhy, Do, (Py), (Qtz)	-
15-11-6-20 W3M 6029	T.W. Eastend Cr. #1	Wymark Upper	Cal, Do, An, (Py), (Qtz)	-
15-11-6-20 W3M 6040	T.W. Eastend Cr. #1	Wymark Upper	Anhy, Do, (Py)	2.8
15-11-6-20 W3M 6053	T.W. Eastend Cr. #1	Wymark Upper	Cal, Do, (Py)	2.8
15-11-6-20 W3M 6059	T.W. Eastend Cr. #1	Wymark Upper	Cal, Do, Anhy, (Py)	9.56
15-11-6-20 W3M 6070	T.W. Eastend Cr. #1	Wymark Upper	Cal, Do, Anhy, (Py)	9.56
15-11-6-20 W3M 6141	T.W. Eastend Cr. #1	Wymark Middle	Cal, Do, An, (Qtz)	9.56
15-11-6-20 W3M 6161	T.W. Eastend Cr. #1	Wymark Middle	Cal, Do, Anhy, (Qtz)	9.56

Cal=calcite, Do=Dolomite, Anhy=Anhydrite, Fl=Fluorite, Py=Pyrite, Qtz=Quartz, Ksp=K-Feldspar, (xx) = trace constituent

Last 4 digits in sample name give the depth in ft.

455

456

457

458 **Figure Captions**

459

460 Figure 1. **(a)** Map showing the location of the Williston Basin and natural CO<sub>2</sub> occurrences  
461 (shown in red) in southwestern Saskatchewan relative to the location of the Weyburn CO<sub>2</sub>  
462 injection site (Lake and Whittaker, 2006). **(b)** Detailed stratigraphy of the Upper Devonian series  
463 in southwestern Saskatchewan.

464

465 Figure 2 - Map indicating the proposed migration pathway of CO<sub>2</sub> generated in Montana through  
466 the contact of alkali magma with limestones approximately 50 million years ago. The locations of  
467 known natural inert gas occurrences in the area are shown along with several basement and intra-  
468 sedimentary structures. Structure contours represent Duperow and equivalent strata in region.

469

470 Figure 3. Structure map of the Duperow Formation displaying the wells from which inert gas  
471 samples high in CO<sub>2</sub> or N<sub>2</sub> have been observed (after Lake and Whittaker, 2006). Of particular  
472 interest are the Eastend (16-11-006020W3, 15-11-006-20W3) and Battle Creek Wells (04-31-03-  
473 26W3).

474 Figure 4. Comparison of the geological setting at the natural CO<sub>2</sub> sites in southwestern  
475 Saskatchewan and the Weyburn injection site. The top diagram depicts the relatively continuous  
476 strata across the intervening distance between the two areas. The detailed geological columns  
477 indicate the broad similarity of geological setting in both areas; the CO<sub>2</sub> is contained in  
478 Palaeozoic carbonate reservoirs capped by anhydrite layers and in turn overlain by approximately  
479 1500 m of Mesozoic shales, siltstones, and sandstones. At the Weyburn site, CO<sub>2</sub> is being  
480 injected into the Mississippian Middle Beds, whereas the naturally occurring CO<sub>2</sub> is found mainly  
481 in the Devonian Duperow Formation in southwestern Saskatchewan.

482

483 Figure 5. (a) Backscattered electron images of 3-10-14-14 W3M 5555 showing euhedral  
484 dolomite grains growing into open porosity. Small grains of fluorite (Fl) appear at the bottom of  
485 the image (b) 4-14-18-16 W3M 4827 Euhedral dolomite and calcite with trace pyrite.

486

487 Figure 6. (a) Backscattered electron images of 5-7-14-10 W3M 5288 showing large calcite grain  
488 almost totally replaced by dolomite. (b) 5-7-14-10 W3M 5413 Dolomite shown replacing calcite.

489 Anhydrite and celestine are the bright sulfate phases.

490

491 Figure 7. (a) Backscattered electron images of 10-32-183 W3M 4596 showing euhedral dolomite  
492 grains associated with anhydrite and fluorite. Anhydrite enclosed fluorite in grain at center of  
493 view. (b) 15-11-6-20 W3M 6014 Dense anhydrite-dolomite assemblage characteristic of aquitard  
494 layers.

495

496 Figure 8. (a) Backscattered electron images of 15-11-6-29 W3M 6161 showing quartz grains. (b)  
497 Quartz in 4-14-18-26 W3M 6014.

498

499 Figure 9. Whole rock compositions of Midale and Duperow samples (Ryerson and Johnson,  
500 2010a, b).

501

502 Figure 10. Electron microprobe analysis of carbonate minerals from the Midale Beds (Durocher  
503 et al., 2003) and the Duperow Formation (Ryerson and Johnson, 2010a, b).

504

505 Figure 11. Zoned dolomite growing into a pore in sample 10-32-183 W3M 4746. This horizon  
506 contained no natural accumulations of CO<sub>2</sub>.

507

508 Figure 12. Histogram of Mg/(Ca+Mg) on a cation basis for the carbonates from the Midale beds  
509 (Durocher et al., 2003) (Durocher et al., 2003 and the Duperow Formation (Ryerson and Johnson,  
510 2010a, b).

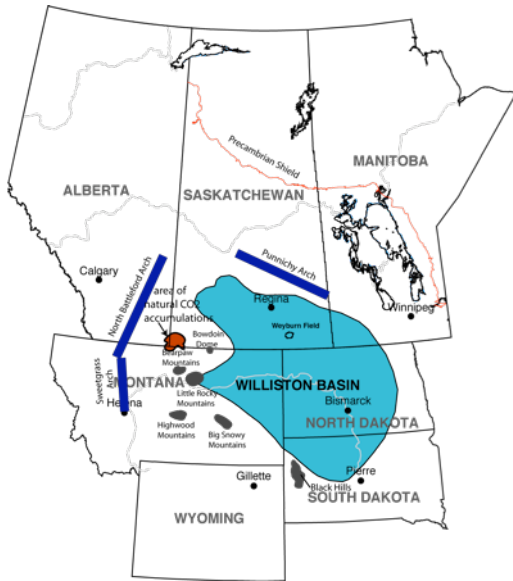
511

512 Figure 13. Porosity data for the (a) Duperow Formation and (b) Midale beds at the Weyburn site.  
513 Midale peak at 0.12 is the Vuggy unit, that at 0.26 is the Marly unit. Data from the Ministry of  
514 Energy and Resources, courtesy of Erik Nickel.

515

516

517  
 518  
 519  
 520  
 521  
 522  
 523  
 524  
 525  
 526

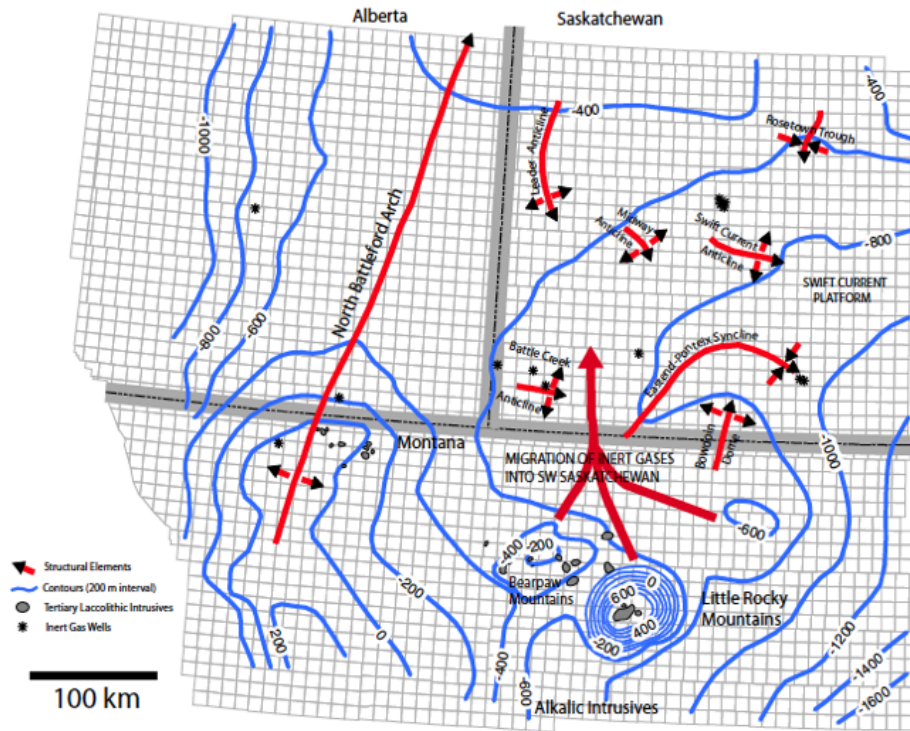


Unit 2	TORQUAY FORMATION	THREE FORKS GROUP
Unit 1		
UPPER MEMBER	BIRDBEAR FORMATION	SASKATCHEWAN GROUP
LOWER MEMBER		
Unit B Subunit B1	SEWARD MEMBER	DUPEROW FORMATION
Unit A		
Upper Unit		
Dinmore Esporte	WYMARK MEMBER	SASKATCHEWAN GROUP
Middle Unit		
Lower Unit		
ELSTOW MEMBER	SASKATOON MEMBER	UPPER DEVONIAN SERIES
SASKATOON MEMBER		
SOURIS RIVER FORMATION	MANITOBA GROUP	

527  
 528  
 529  
 530  
 531  
 532

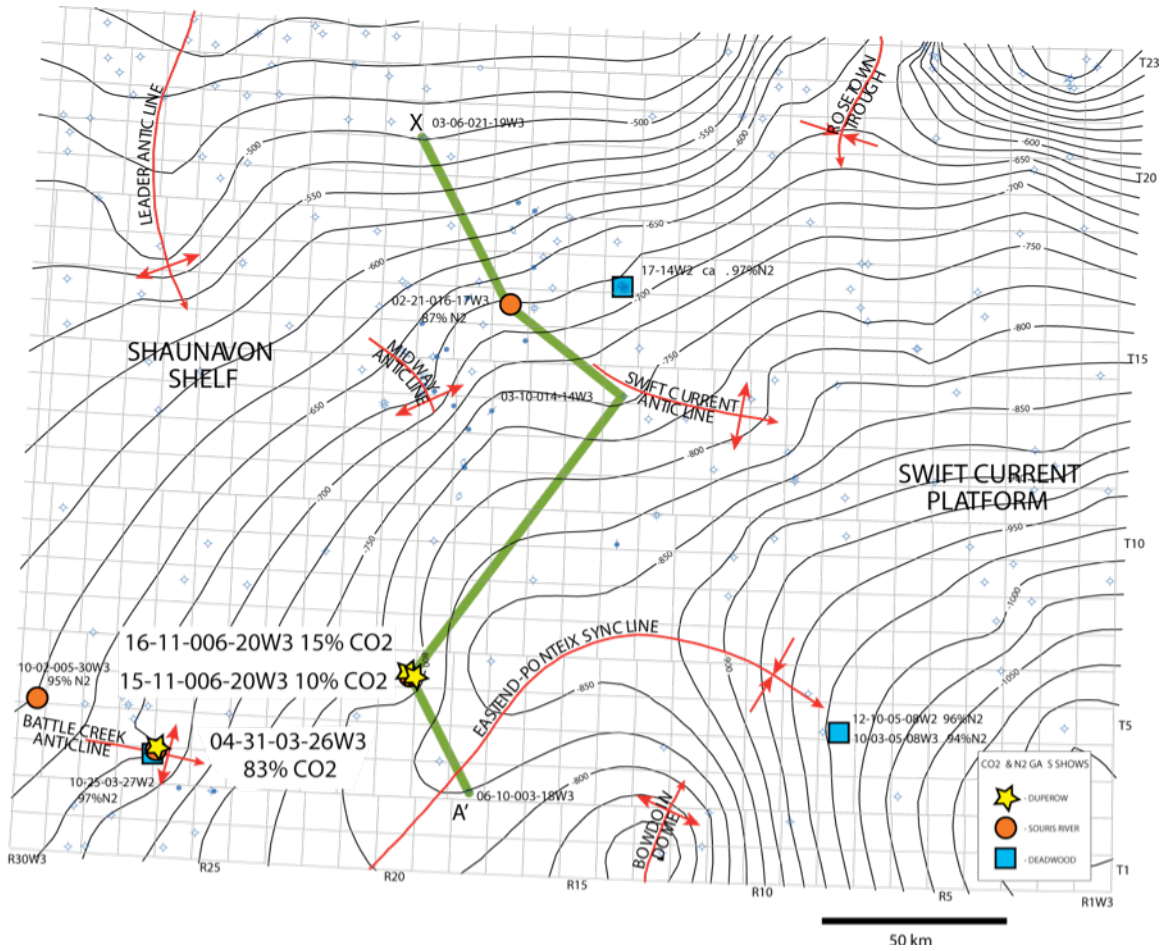
Figure 1

533  
534  
535  
536  
537



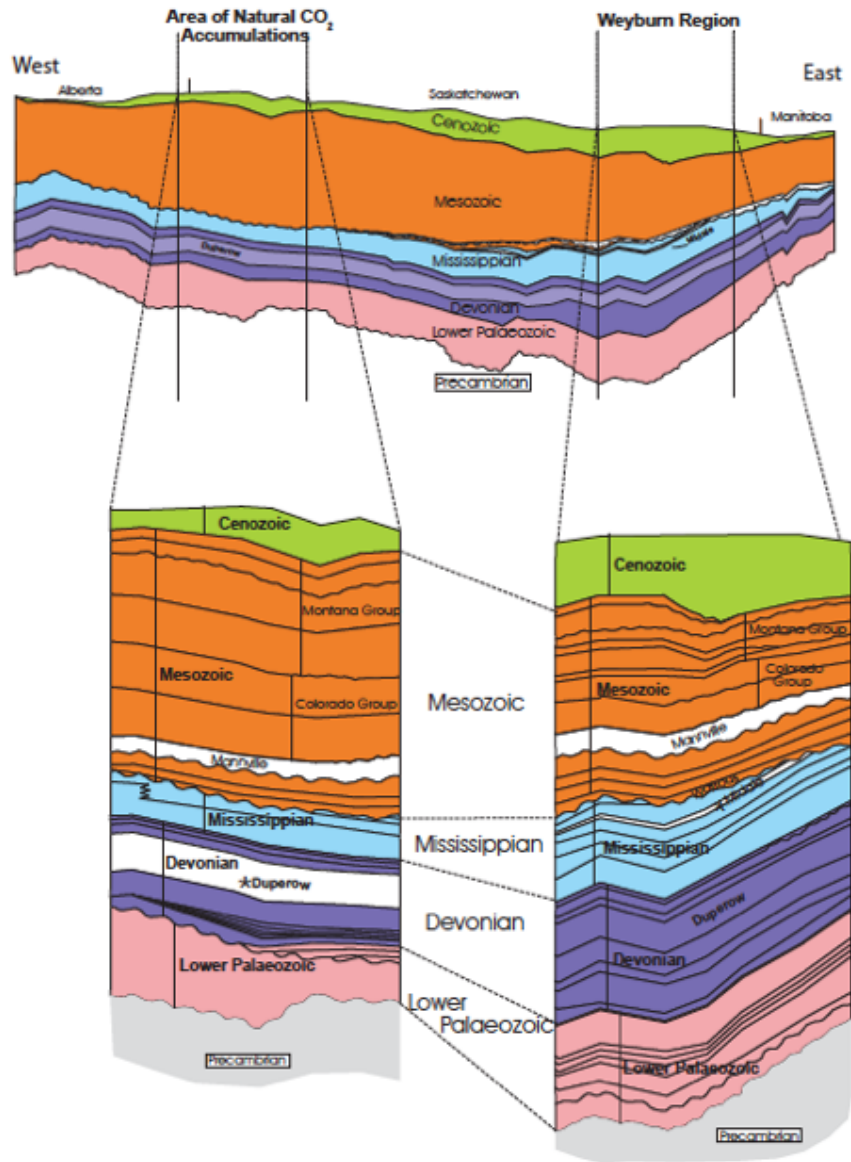
538  
539 Figure 2  
540

541  
542  
543  
544  
545  
546  
547  
548  
549



550  
551  
552  
553

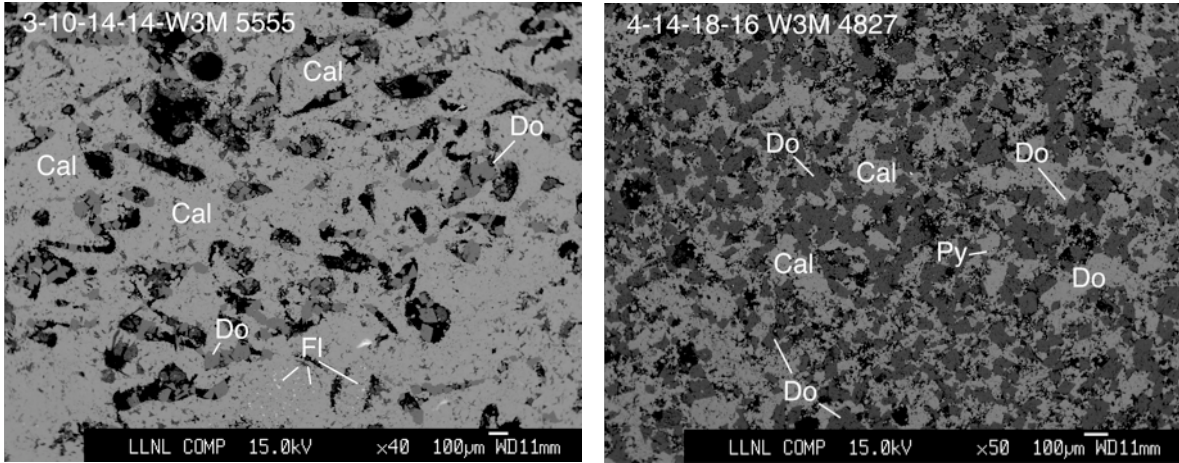
Figure 3



554  
 555  
 556  
 557  
 558

Figure 4

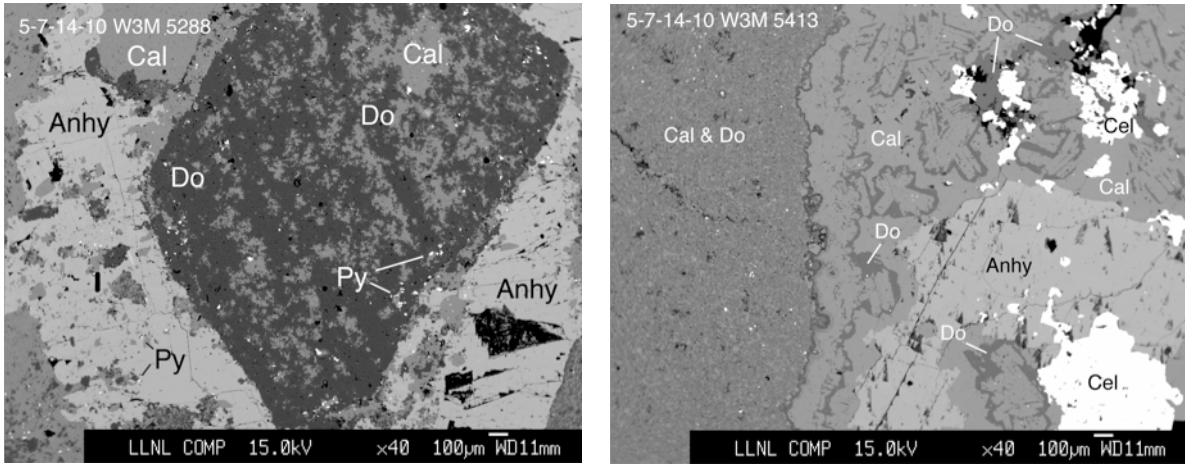
559  
560  
561  
562  
563



564  
565  
566  
567  
568  
569

Figure 5

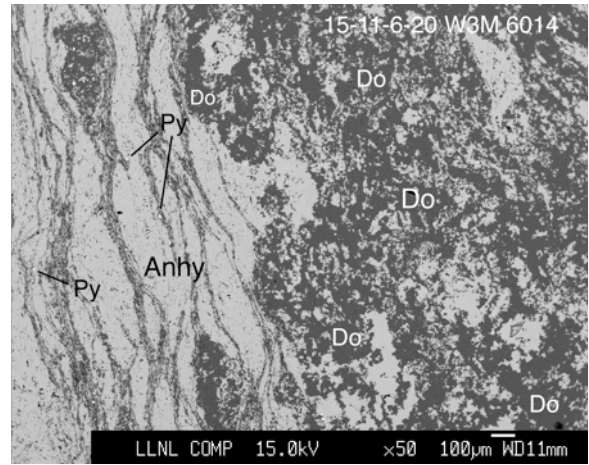
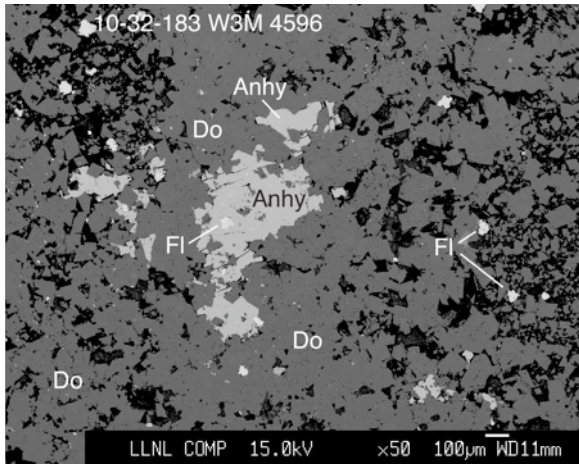
570  
571  
572  
573  
574



575  
576  
577  
578

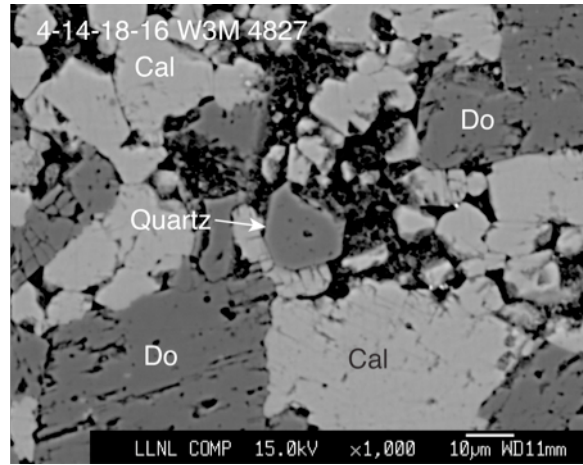
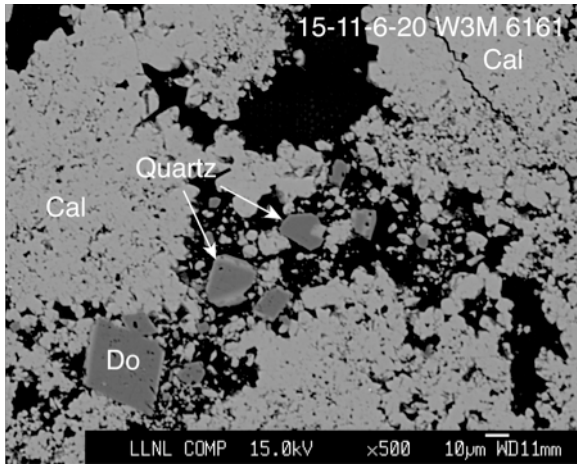
Figure 6.

579  
580  
581  
582



583  
584 Figure 7

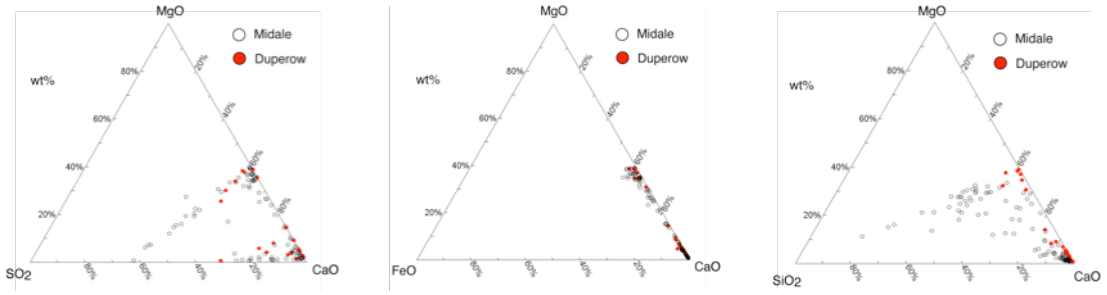
585  
586  
587  
588



589  
590  
591

Figure 8

592  
593

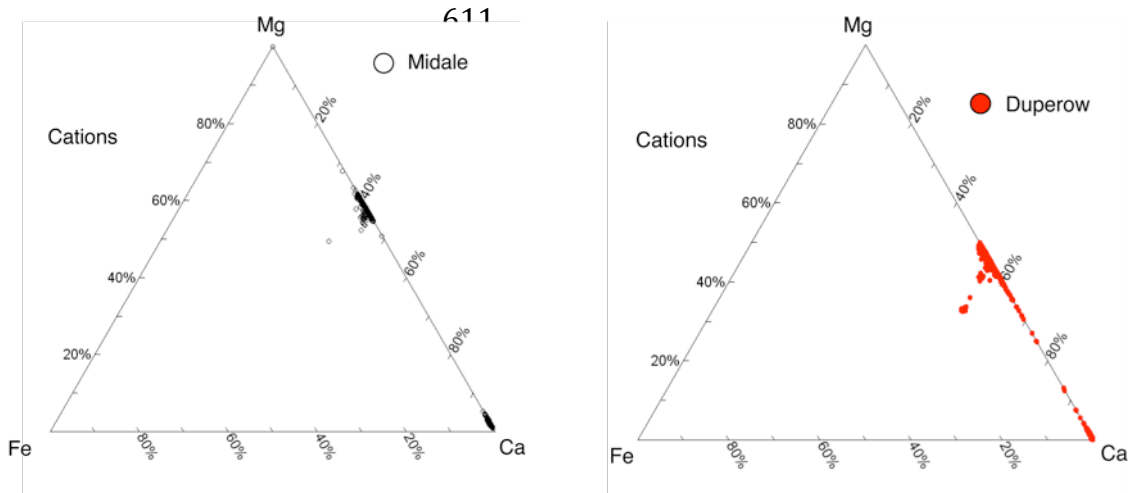


594  
595  
596  
597  
598  
599

Figure 9

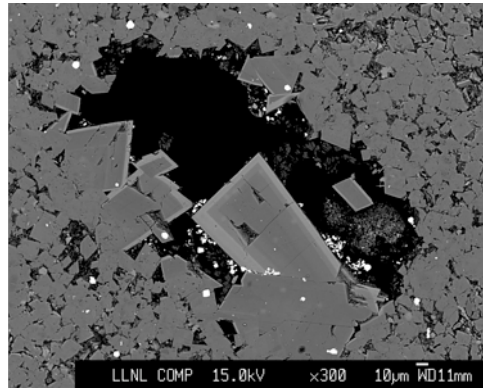
600  
601  
602  
603  
604

605  
606  
607  
608  
609  
610



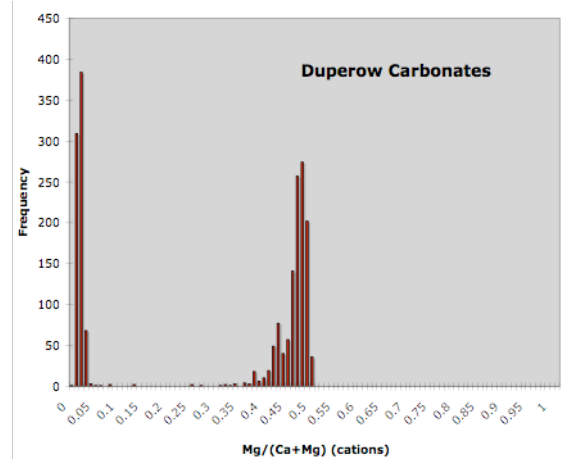
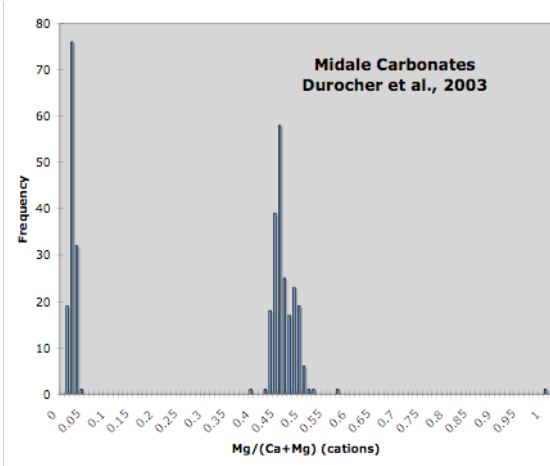
616 Figure 10  
617

618  
619  
620  
621  
622



623  
624 Figure 11  
625  
626

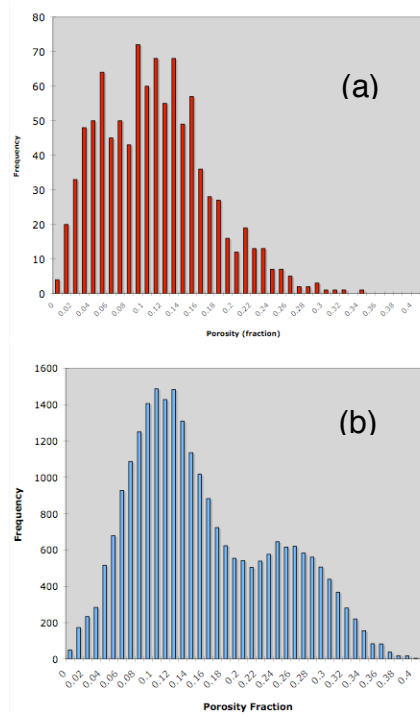
627  
628



629

630 Figure 22  
631  
632

633  
634



635  
636  
637 Figure 13  
638  
639